RSC Advances

ROYAL SOCIETY OF CHEMISTRY

www.rsc.org/advances

ARTICLE

Density functional theory study of hydrogenation of S to H_2S on Pt-Pd alloy surfaces

Yunjie Liu, [a] Wei Gao,[a] Guixia Li,[a] Yahui Guo,[a] Jun Zhu[b], Lanzhong Hao,[a*]

Received 00th January 2015,
Accepted 00th January 2015

DOI: 10.1039/x0xx00000x
www.rsc.org/

In this work, the adsorption of S-containing species (S, HS, and H_2S) and the hydrogenation of S on the Pt-Pd alloy were investigated by using the periodic density functional theory(DFT). The energy minimum of the adsorbed S, HS, and H_2S were identified to bind preferentially on the fcc, bridge and top sites, respectively. Compared to single metal surfaces, the adsorption energies of adsorbates were calculated to be larger on the Pt-Pd alloy surfaces and adsorbed preferably on the sites with a majority of Pt atoms. The reaction pathways and energy profiles for the conversion of adsorbed S and H into gas phase H_2S were determined. The results showed that both the S+H and HS+H reactions on Pt-Pd alloy surfaces were endothermic. The energy for the overall reaction on Pt-Pd alloy surfaces decreased significantly by 0.30～0.55 eV compared to pure Pt(111) surface. In addition, the energy barrier on Pt-1Pd(111) (one Pt atom was replaced by Pd atom on Pt(111) surface) was lower than that on other studied alloy surfaces. The above characteristics revealed that the hydrogenation of S to H_2S was easier on Pt-1Pd(111) surface than on the other alloy surfaces. The partial density of states was utilized to illustrate the interaction mechanisms between S-containing species and surface atoms .

1. Introduction

Platinum catalysts have received much attention due to their high activity towards the hydrodesulfurization (HDS) of organic sulfur compounds and their wide application in the area of the petrochemical processes.[1] However, the catalysts could be easily poisoned and deactivated under sulfuric conditions. The previous studies indicated that sulfur containing molecules in feedstock, even in small levels of S impurities, can drastically reduce the catalytic efficiency of transition metal surfaces.[2-4] Therefore, many attempts have been made to enhance sulfur resistance of platinum catalysts. Recent studies show that the addition of a second transition metal into platinum catalysts may effectively improve catalytic activity and sulfur resistance.[5, 6] In particular, Pt-Pd alloy catalysts have received a lot of attention since they have exhibited superior sulfur resistance.[7-10] The Pt-Pd alloy catalysts perform better than either of the monometallic catalysts in selectivity, activity as well as resistance to poisoning. Lee et al. investigated the sulfur tolerance of bimetallic Pd-Pt/H-Beta catalysts for the isomerization of *n*-hexane in the presence of thiophene.[11] The results showed that Pd-Pt/H-Beta catalysts were more sulfur resistant than Pd/H-Beta and Pt/H-Beta, regardless of the preparation method and the Pd-Pt atomic ratio. This suggests that the Pt-Pd bimetallic interaction could increase the amount of electron-deficient metal sites and the sulfur tolerance could be enhanced due to the reduction of the irreversible electrophilic sulfur adsorption. Yasuda et al. confirmed that tetralin hydrogenation could be enhanced largely due to the coexistence of Pt and Pd. The high sulfur tolerance of the Pt-Pd system could be attributed to the structural and electronic effects.[12] Niquille-Röthlisberger et al. thought that high hydrogenation activity of Pt-Pd alloy catalysts originated from the new active sites in the Pt-Pd catalysts.[13]

In spite of large quantities of experimental works about the Pt-Pd alloy catalysts, to our knowledge, little theoretical work has been carried out. Jiang et al. studied the adsorption of S, HS and H_2S on Pt-Pd alloys metal.[14] They thought the structure changes in Pt-Pd bimetallic catalysts gave rise to different active sites that made the adsorption of H_2 more competitive to the adsorption of H_2S and S. However, little is known about electron structure of S on the different active sites and the mechanism of hydrogenation reaction of S on Pt-Pd alloy surfaces. Undoubtedly, it is important to understand these elementary reactions for a number of industrial processes. In this paper, the hydrogenation reactions of sulfur were examined with density functional theory (DFT) to determine the catalytic effect of alloying Pt with Pd on the Pt-Pd catalysts. The optimized adsorption configurations, adsorption energies and partial density of states (PDOS) analyses of S, HS, H_2S and H were presented. The main reaction pathways were obtained on the targeted metal surfaces.

2. Computation details

The calculations were performed in the framework of DFT with program package DMol^3 and CASTEP in Materials Studio of Accelrys Inc.[15-17] The exchange-correlation energy was calculated within the generalized gradient approximation (GGA) using the form of the function proposed by Perdew and Wang, usually referred as to Perdew-Wang 91.[18,19] The PW91 functional has the shortcoming that does not contain dispersion contribution to some systems, but

[a] *College of Science, China University of Petroleum, Qingdao, Shandong 266580, People's Republic of China. E-mail: haolanzhong@upc.edu.cn*
[b] *State Key Laboratory of Electronic Thin Films and Integrated Devices, University of Electronic Science and Technology of China, Chengdu 610054, People's Republic of China.*

the contribution of van der Waals (vdW) dispersion term is small. Garćla-Muelas et al. reported that the inclusion of vdW interactions could enhance the adsorption energies by 0.01-0.20 eV using applying Grimme's DFT-D2 method for the reavtants, products and decomposition on Cu, Ru, Pd and Pt surfaces.[20] Furthermore, we calculated the adsorption energy of H adsorption at the top site on Pt(111) with the PBE exchange-correlation functional. The adsorption energy (2.77 eV) were almost equal with the energy (2.80 eV) calculated with PW91 functional, suggesting that dispersion effects have little influence to the results.

The density functional semicore pseudopotential (DSPP) method was employed for the metal atoms,[21] and the all-electron basis set was used to treat the incorporated atoms, such as H and S atom. The valence electron functions were expanded into a set of numerical atomic orbital by a double-numerical basis with polarization functions (DNP). A Fermi smearing of 0.136 eV was used to improve the computational performance. Spin-polarization was performed during the whole computations.

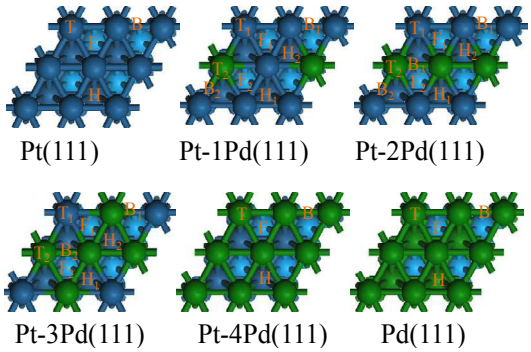

Fig. 1. Illustration of adsorption sites on Pt-nPd (111) surface in the top view. T, T_1 and T_2 denote top sites; B, B_1, B_2 and B_3 denote bridge sites; F, F_1 and F_2 denote fcc sites; H, H_1 and H_2 denote hcp sites. Blue and green represent Pt atoms and Pd atoms in the first layer.

Here, we choose the (111) of Pt as the initial surface because it is the most stable crystal planes in the exposed basal planes of nanoparticles. The Pt(111) surface is modelled using a four-layer slab model with four atoms per layer representing a (2×2) surface unit cell and a 14 Å vacuum region. The reciprocal space is sampled by a grid of (5×5×1) k-points generated automatically using the Monkhorst-Pack method.[22] A single adsorbate is allowed to adsorb on one side of the (2×2) unit cell, corresponding to a surface coverage of 1/4 ML. Full-geometry optimization is performed for all relevant adsorbates and the upper most two layers without symmetry restriction, while the bottom two layer Pt atoms are fixed to their calculated bulk positions. The tolerances of energy, gradient, and displacement convergence are 1.0×10^{-5} Hartree, 2.0×10^{-3} Hartree/Å, and 5×10^{-3} Å, respectively. In order to study the alloy effects, Pt atoms on the first layer of the Pt(111) surface are replaced by Pd atoms as our computational models, which are described as Pt-nPd(111) (n=1-4). The atomic ratio between Pt and Pd on the first layer was thus 3/1, 2/2, 1/3, and 0/4, respectively. The computational model is in consistent with previous work.[14] The Pd(111) model is built of all the Pd atoms , using a four-layer slab model with four atoms per layer representing a (2×2) surface unit cell and a 14 Å vacuum region. The slab models of Pt(111), four kinds of bimetallic surfaces and the Pd(111) are shown in Fig. 1. On the (111) facet of a face-centered cubic structure, the surface sites include top (T), bridge (B), fcc (F), and hcp (H), only one equivalent site for the adsorption of species on each of the T, B, F, and H sites on Pt(111), Pd(111), and Pt-4Pd(111), while on the other alloy surfaces, each of these sites can be classified into two or three catalogs, differentiated by footnotes 1, 2, and 3, in which the smaller footnote number denotes the corresponding site is relevant to more Pt atoms, while the situation of the larger footnote number is the reverse.

The bulk lattice constants and adsorption energies were calculated to ensure the reliability of the computational results. The calculated lattice constant of the bulk Pt and Pd were 4.006 and 3.983 Å, respectively, which are in good agreement with the experimental values (3.912 and 3.883 Å)[23, 24] and other theoretical values (3.971 and 3.965 Å).[25, 26] The adsorption energies of H adsorbed on Pt(111) and Pd(111) were calculated. H can adsorb at all site on Pt(111) with a similar energy, with 2.80 eV at the T site, 2.71 eV at the F site, 2.68 eV at the H site and 2.71 eV at the B site. The results agree very well with previous calculations.[27] On Pd(111), The most favourable site for H is found to be at the F site and the adsorption energies are calculated to be 2.82 eV. The result are in very good agreement with previous experimental study (2.80 eV).[28]

The adsorption energies reported here were calculated using the equation:

$$E_{ads} = E_{adsorbate} + E_{slab} - E_{adsorbate/slab} \quad (1)$$

Where E_{ads} is the adsorption energy of the adsorbate on the metal surface, $E_{adsorbate/slab}$ is the energy of the adsorbate/slab adsorption system, $E_{adsorbate}$ and E_{slab} are the energies of the free adsorbate and the clean slab, respectively. A positive value of E_{ads} indicates a stable adsorption by this definition.

Transition state (TS) searches were performed at the same theoretical level with the complete LST/QST method.[15,16,29] Vibrational frequencies were calculated for all the initial state (IS) and final state (FS) as well as the TSs from the Hessian matrix with the harmonic approximation. The zero-point energy (ZPE) was calculated from the resulted frequencies. The reaction energy (ΔE) and energy barrier (E_a) of a step on Pt-Pd alloys can be calculated by the following formulas,

$$\Delta E = E_{FS} - E_{IS} \quad (2)$$

$$E_a = E_{TS} - E_{IS} \quad (3)$$

Where E_{IS}, E_{TS} and E_{FS} are the total energies of the initial state (IS), transition state (TS), and final state (FS), respectively. Rate constant k can be estimated using conventional transition state theory.[30]

$$K = \frac{k_B T}{h}\frac{Q_{TS}}{Q_{IS}} e^{-(E_a/K_B T)} = A^{\circ} e^{-(E_a^{\circ}/K_B T)} \quad (4)$$

Where k_B and h are the Boltzmann constant and the Planck's constant, respectively; Q_{IS} and Q_{TS} are the partition functions at the IS and TS, respectively; E_a° and E_a are energy barriers with and without ZPE corrections; T and A° are the temperature and the pre-exponential factor, respectively.

3. Results and Discussion

This part is divided into four sections. In section 3.1, the structures of metal surfaces are described. In section 3.2, the adsorptions of S and surfaces species involved are discussed. In section 3.3, electronic states of adsorption structures are analyzed. In section 3.4, the reaction paths of the hydrogenation of S are elaborated.

3.1 Structures of metal surface

The geometric and electronic structures of the surfaces with different Pt/Pd ratios are calculated and the obtained parameters are summarized in Table 1. The Pt(111) surface is flat with the distance of 2.38 Å between the most upper two layers. After Pd doping, due to the difference of lattice constant, the surface Pt atoms move inward by 0.02~0.08 Å and the Pd atoms yield a height of about 0.10 Å higher than the surrounding Pt atoms. The distance of the first and second layer Pt-Pt in pure Pt(111) is 2.875 Å. After Pd doping, the Pt-Pt bonds are shortened about 0.02~0.07 Å and the distance of Pt-Pd decreases from 2.916 to 2.845 Å with the increasing of the Pd number. Furthermore, the electrons transfer from Pd to Pt in the upper layer due to their different electronegativities. The transferred charges of Pt atom increase with increasing of the Pd atoms. The Pt atoms of the second layer get electron after Pd atoms doping. The overlap population values in Table 2 indicates the interactions in the upper layer are more strongly covalent than the first-second interlayer bonds, which are weakly covalent (Pt-Pt) or antibonding (Pd-Pt) interactions. The covalent components of the bonds in the uppermost layer follows the order of Pt-Pt (0.54~0.75) > Pt-Pd (0.24~0.45) > Pd-Pd (0.04~0.34), and the values for each type of the bonds increase with increasing the alloying atom number. These results are well consistent with the results of the corresponding bond lengths.

Table 1. Atomic charges for surface Pt, Pd, 2nd layer Pt atom and the distance of Pt-Pt/Pd on first and second layer.

System	Atom	Charge	$d_{Pt\text{-}Pt/Pd}$ (Å)	
			$Pt\text{-}Pt_a/Pd\text{-}Pd_a$	$Pd\text{-}Pt_a$
Pt	Pt	-0.016	2.875	
	Pt_a	0.013		
Pt-1Pd	Pt	-0.068	2.851	2.916
	Pd	0.190		
	Pt_a	0		
Pt-2Pd	Pt	-0.122	2.828	2.894
	Pd	0.148		
	Pt_a	-0.014		
Pt-3Pd	Pt	-0.180	2.808	2.865
	Pd	0.099		
	Pt_a	-0.030		
Pt-4Pd	Pd	0.047		2.845
	Pt_a	-0.048		
Pd	Pd	-0.013	2.842	
	Pd_a	0.011		

a second layer Pt or Pd atoms. Pd is nearest the site of S atom.

The partial density of states (PDOS) for metal surfaces is shown in Fig. 2. We find that with the increase of the Pd atoms (1) the range of the PDOS is successfully narrowed, i.e., from -13.0 eV to -5.87 eV for Pt(111) to -10.2 eV to -5.22 eV for Pd(111); (2) the Fermi level is higher located, that is, -5.87 eV for Pt(111) to -5.22 eV for Pd(111).

3.2 Adsorptions of the S hydrogenation intermediates

To explore the hydrogenation of S, the preferential adsorption site for S, HS, H_2S and H should be determined firstly. In this section, the adsorption geometries of all the intermediates are described. Table 3 lists some important parameters for these intermediates, and the most stable adsorption configurations are shown in Fig. 3.

Table 2. Overlap population (OP) values on metal surface

system	surface			1^{st}-2^{nd} layer		
	Pt-Pt	Pt-Pd	Pd-Pd	$Pt\text{-}Pt_a$	$Pd\text{-}Pt_a$	$Pd\text{-}Pd_a$
Pt(111)	0.54			0		
Pt-1Pd(111)	0.65	0.24		0.06	-0.09	
Pt-2Pd(111)	0.75	0.35	0.04	0.11	-0.05	
Pt-3Pd(111)		0.45	0.14	0.12	-0.02	
Pt-4Pd(111)			0.23		0.03	
Pd(111)			0.34			-0.01

a second layer Pt or Pd atoms. Pd is the closest to S atom.

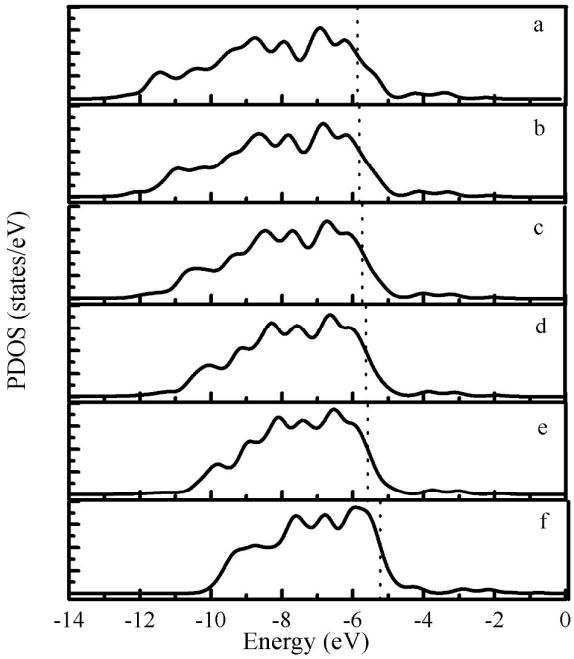

Fig. 2. PDOS for different clean surfaces: (a) Pt(111), (b) Pt-1Pd(111), (c) Pt-2Pd(111), (d) Pt-3Pd(111), (e) Pt-4Pd(111), (f) Pd(111)

S: On the studied metal surfaces, adsorption of S in all these possible sites is considered, and only the H and F sites are found to be stable adsorption sites, with the F sites being more stable than the corresponding H sites by 0.03~0.15 eV. Although on Pt(111) and Pd(111), the adsorption energy is almost the same (4.45 vs 4.42 eV), substitution of the surface Pt with Pd strengthens adsorption of S at the F_1 site on Pt-nPd(111) (n=1-4) (4.59~4.69 eV). This is consistent with the previous theoretical work.[14] The adsorption energy decreases at both F_1 and F_2 sites with increasing Pd number (n =1-3), and the difference of the energies at the F_1 and F_2 sites is enlarged from 0.23 to 0.31 eV. It is interesting to note that the full surface alloying gives the largest adsorption energy of atomic S (4.69 eV). Although the S-metal bonds on Pt(111) is longer than on Pd(111), surface alloying results in the shortening the S-Pt bond and the stretching of the S-Pd bond as compared to the values of the respective pure surfaces. On the same alloy surface, the S-Pt bond length is shorter than the S-Pd distance, reflecting the stronger adsorption strength.

We also study the S adsorption when H absorbed the surface. The adsorption energy on Pt(111), Pt-1Pd(111), Pt-2Pd(111), Pt-3Pd(111), Pt-4Pd(111) and Pd(111) are 4.31, 4.30, 4.29, 4.25, 4.22 and 3.89 eV, respectively. The adsorption energies are 0.14~0.53 eV less stable than that only S adsorb on the metal surface, indicating a slight repulsive interaction between S and H. Our main goal in this work is to describe the potential energy surface (PES) of the hydrogenation reaction to compare the reaction rate on the different metal surface. So we think the effect is very small.

HS: HS is a short-lived catalytic intermediate and it is difficult to be observed and characterized experimentally.[25] A theoretical approach is, therefore, necessary to study the reaction intermediates. This can present the high scientific information about the structures and energetics of the adsorption configurations. Our calculations reveal that all types of B sites are possible for HS, in which the H-S bond is inclined to the surface normal (99.3~106.0°) with the S atom at the B site. For Pt-nPd(n=1-3), the B_1 site is always most preferable. Different from the

Table 3. Geometric and energetic parameters of the stable adsorption structures for adsorbates on the studied metal surfaces

species	slab	sites	E_{ads}(eV)	$d_{S\text{-}Pt}$(Å)	$d_{S\text{-}Pd}$(Å)	$d_{S\text{-}H}$(Å)	angles[a](°)
S	Pt	F	4.45	2.322, 2.322, 2.323			
		H	4.30	2.326, 2.329, 2.339			
	Pt-1Pd	F_1	4.67	2.315, 2.317, 2.318			
		H_1	4.52	2.323, 2.323, 2.324			
		F_2	4.43	2.302, 2.303	2.344		
		H_2	4.31	2.305, 2.305	2.355		
	Pt-2Pd	F_1	4.65	2.300, 2.301	2.337		
		H_1	4.53	2.304, 2.306	2.337		
		F_2	4.37	2.289	2.325, 2.326		
		H_2	4.28	2.284	2.332, 2.333		
	Pt-3Pd	F_1	4.59	2.281	2.325, 2.323		
		H_1	4.49	2.284,	2.332, 2.333		
		F_2	4.28		2.308, 2.308, 2.309		
		H_2	4.21		2.310, 3.211, 2.313		
	Pt-4Pd	F	4.69		2.304, 2.305, 2.306		
		H	4.66		2.310, 2.312, 2.315		
	Pd	F	4.42		2.301, 2.304, 2.306		
		H	4.34		2.308, 2.308, 2.309		
HS	Pt	B	2.31	2.380, 2.378		1.377	104.3
	Pt-1Pd	B_1	2.77	2.371, 2.370		1.376	106.0
		B_2	2.57	2.353	2.430	1.373	102.2
	Pt-2Pd	B_1	2.89	2.364, 2.364		1.377	99.4
		B_2	2.72	2.348	2.414	1.376	101.2
		B_3	2.50		2.380	1.372	101.6
	Pt-3Pd	B_1	2.86	2.340	2.405	1.376	104.4
		B_2	2.64		2.378, 2.379	1.373	103.3
	Pt-4Pd	B	2.78		2.368, 2.368	1.376	99.3
	Pd	B	2.49		2.373, 2.368	1.377	102.5
H_2S	Pt	T	0.77	2.387		1.367	91.4
	Pt-1Pd	T_1	0.80			1.367	91.2
		T_2	0.67	2.372	2.444	1.361	91.6
	Pt-2Pd	T_1	0.83	2.358		1.367	91.1
		T_2	0.71		2.417	1.362	91.6
	Pt-3Pd	T_1	0.88	2.346		1.368	91.1
		T_2	0.75		2.201	1.364	91.2
	Pt-4Pd	T	0.80		2.373	1.365	91.2
	Pd	T	0.74		2.386	1.366	91.5

[a]Values are angles between the surface normal and the H-S axis when HS adsorption and the H-S-H angles when H_2S adsorption

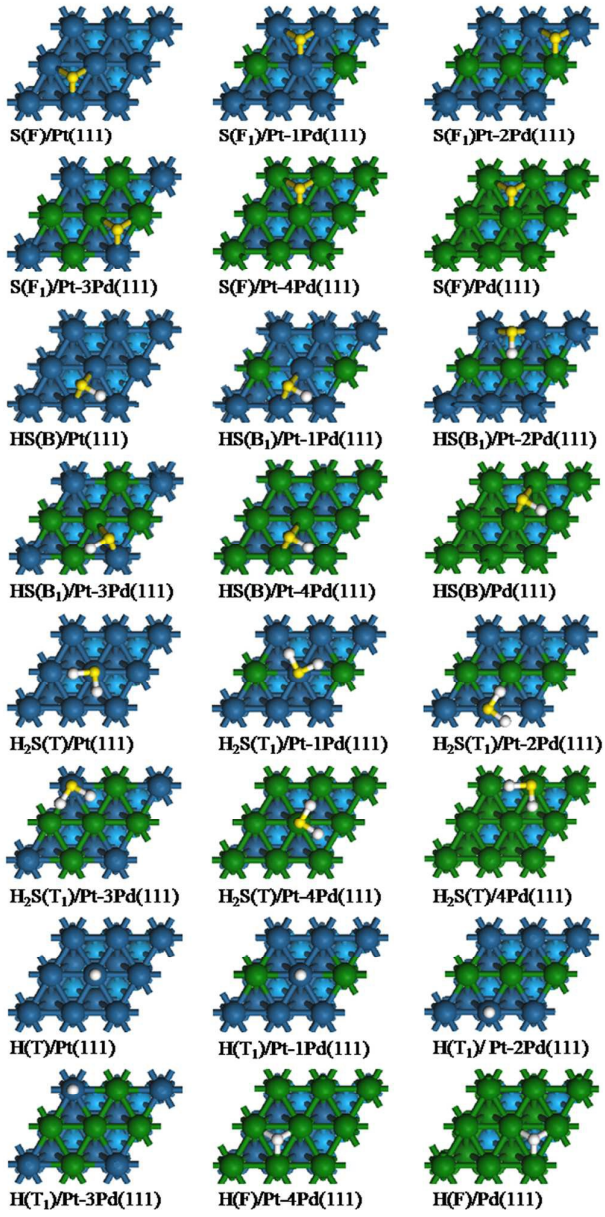

Fig. 3. The most stable adsorption structures of adsorbates on the metal surfaces.

situation of atomic S, the pure crystal surfaces of Pt and Pd account for relatively large difference in the adsorption energies for HS, i.e., 2.31 and 2.49 eV, respectively. Surface alloying strengthens its interaction with HS compared to the situation any of the pure surfaces, but to different extents for different alloying and different bridge sites, i.e., 2.77 and 2.57 eV on the B_1 and B_2 site on Pt-1Pd(111); 2.89, 2.72 and 2.50 eV on the B_1, B_2 and B_3 site on Pt-2Pd(111); 2.86 and 2.64 eV on the B_1 and the B_2 site on Pt-3Pd(111); 2.78 eV on Pt-4Pd(111). Thus, one more Pd atom involved in the B site results in ~0.2 eV decrease in the adsorption energy.

Table 4. The stable adsorption configuration, adsorption energies and structural parameters of H on the Pt(111), Pd(111) and Pt-nPd alloy surface.

species	sites	E_{ads}(eV)	$d_{H\text{-}Pt}$(Å)	$d_{H\text{-}Pd}$(Å)
Pt	T	2.80	1.554	
	F	2.71	1.872, 1.876, 1.879	
	H	2.68	1.873, 1.878, 1.880	
	B	2.71	1.751, 1.761	
Pt-1Pd	T_1	2.83	1.555	
	T_2	2.28		1.538
	F_1	2.76	1.867, 1.872, 1.895	
	H_1	2.70	1.875, 1.879, 1.889	
	F_2	2.78	1.796, 1.808	2.050
	H_2	2.76	1.786, 1.788	2.144
	B_1	2.77	1.758, 1.760	
	B_2	2.71	1.667	1.921
Pt-2Pd	T_1	2.86	1.556	
	T_2	2.33		1.541
	F_1	2.82	1.794, 1.807	2.074
	F_2	2.81	1.724	1.932, 1.960
	H_2	2.79	1.708	1.958, 1.985
	B_1	2.82	1.759, 1.759	
	B_2	2.78	1.668	1.918
Pt-3Pd	T_1	2.89	1.559	
	T_2	2.36		1.543
	F_1	2.86	1.715	1.955, 1.956
	F_2	2.77		1.821, 1.821, 1.822
	H_1	2.81	1.704	1.967, 2.008
	H_2	2.76		1.821, 1.824, 1.827
Pt-4Pd	T	2.40		1.551
	F	2.82		1.822, 1.822, 1.826
	H	2.78		1.826, 1.831, 1.832
Pd	T	2.42		1.546
	F	2.82		1.814, 1.814, 1.816
	H	2.76		1.814, 1.822, 1.824

Structurally, the S-H bonds in all cases are very similar, 1.372~1.377 Å, irrespective of the large difference in adsorption energies. This value is close to the value (~1.360 Å) for the gas phase. On pure metal surfaces, the S-Pt distance (~2.380 Å) is a little larger than the S-Pd distance (~2.370 Å), surface alloying results in the tendency of shortening the S-Pt distance as well as stretching the S-Pd distance. HS was observed on Pt(111) by HREELS to be stable on the surface up to 150 K.[31] It was suggested that HS may be inclined on Pt(111) based on the HREELS analysis.

H_2S: H_2S has a bent structure with the lone-pair electrons on the S atom, the S-H bond lengths are calculated to be 1.355 Å (1.328 and 1.350 Å), the H-S-H angle is 91.2˚ (92.2 and 91.6˚), in excellent agreement with the previous calculated and experimental values in the parentheses.[32-35] On the metal surfaces, our calculations denote that H_2S preferentially adsorbs via the S atom on the top sites of the surfaces favoring a parallel configuration, in which one of the H atom points to an adjacent surface atom and the other to a hollow site. Placed initially at any other high symmetry sites, H_2S can be diffused to the nearest top site upon geometry relaxation in agreement with previous studies.[25, 36] On the Pt(111), Pt-4Pd(111) and Pd(111) surface, only the T site is possible for H_2S, and the adsorption energies are 0.77, 0.80 and 0.74 eV, respectively. On Pt-nPd(111) (n=1-3) surface, however, H_2S is found to adsorb on the T_1 and T_2 sites, and the T_1 site is more favorable, no matter what the Pt and Pd atomic ratio is. The adsorption energy shows the increase tendency with increasing of the Pd to Pt ratio, from 0.80 eV for Pt-1Pd(111) to 0.83 eV for Pt-2Pd(111) and to 0.88 eV for Pt-3Pd(111); the same variation tendency of the adsorption energy is also followed for H_2S on the T_2 site. The H-S-H internal angles and H-S bond lengths change slightly, with H-S-H internal angles of 91.1 ~ 91.4˚ and bond lengths of 1.365~1.368 Å on the T_1 site for the Pt-nPd(111)(n=0-4), respectively, suggesting that the incorporation of Pd atoms has almost no effects on the structure of H_2S. The H-S distances are stretched and the H-S-H angles are barely changed comparing with the values in vacuum. The calculation shows that the adsorption energies of the S-containing species in their most stable configuration on studied metal surface decrease in the following sequence: S > HS > H_2S.

H: To determine possible reaction states, the adsorption of H is calculated on the metal surface . The stable adsorption energies are listed in Table 4. We find that H is capable of binding at all sites on the surfaces studied, except for the B sites on Pt-3Pd(111), Pt-4Pd(111) and Pd(111). On Pt(111), it is found that H has a very smooth potential energy surface with the small variations of adsorption energies, about 0.1 eV, and the T site is preferred. These results are in good agreement with experimental[37] and other DFT studies.[38] On the Pt-4Pd(111) and Pd(111) surfaces, the most stable adsorption of H is the F site with the adsorption energy of 2.82 eV. On Pt-nPd(111) (n=1-3), the adsorption energies are very close to each other except for T_2 site, with the T_1 site being the most favorable (E_{ads}=2.83~2.89 eV). This demonstrates that atomic H can diffuse readily on the surface. The significant mobility of adsorbed H is expected to favour the hydrogenation process. The adsorption energy for Pt-nPd(111) (n=1-3) increases with increasing the number of Pd atoms. The bond lengths of Pt-S for the are small change, and the preferred adsorption are 1.822 and 1.814 Å for Pd-S on Pt-4Pd(111) and Pd(111), respectively.

3.3 Electronic structure

To clarify the surface alloying effect, PDOS for adsorbed S, HS and H_2S was analyzed. Since Pt-nPd(111) (n=1-3) show similar adsorption effect, i.e., the F_1 site is more stable than F_2 for S and the T_1 site is more stable than T_2 for H_2S on the different alloy surfaces. For simplicity, we discuss only the PDOS of S, HS and H_2S adsorbed on Pt-1Pd surface. PDOS for S adsorbed on the F_1 and F_2 sites was analyzed as shown in Fig. 4. After S adsorption, d states of Pt or Pd atom spread out into lower energies and broaden, where the electron density overlaps with the p states of S. The density of d states of Pt or Pd atom close to the Fermi level is

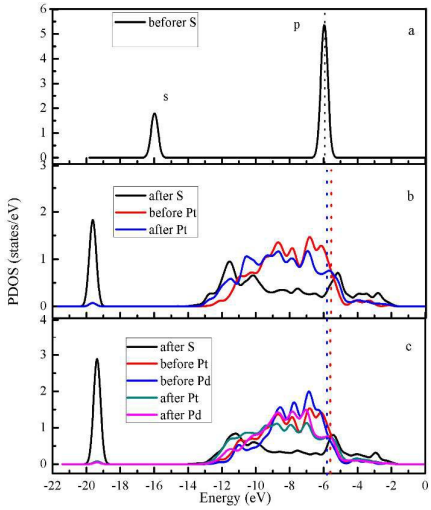

Fig. 4. Partial density of states (PDOS) of S adsorption on Pt-1Pd(111): (a) isolated S, (b) S at the F_1 site, (c) S at the F_2 site.

reduced relative to the before adsorption. These results indicate rehybridization of the surface atoms d states and the S atom p states form strong covalent bonds. In Fig. 4c, the two overlap areas of the density of states of the F_1 located at around -11.5 and -19.7 eV, respectively, are lower than those of the F_2 counterparts (Fig. 4c, at around -11.2 and -19.4 eV, respectively), indicating a stronger interaction between the S and surface atom result in a larger adsorption energy of when S is adsorbed at the F_1 site. The overlap population values of S at the F_1 and F_2 sites on Pt-1Pd(111) surface as shown in Table 5. The overlap population value for Pt-Pt and Pt-Pd bonds on the first layer decrease when S is adsorbed on the first layer decrease when S is adsorbed on the pt-1Pd(111) surface. This suggests that the Pt-Pt and Pt-Pd bonds of the surface weakened due to the adsorption of S atom. The Pt-S bond is stronger than Pd-S bond as shown the overlap population value when S adsorb at the F_2 site. The result is agreed with the bond length (0.53 for Pt-S and 0.27 for Pd-S).

Table 5. Overlap population (OP) values of S at F_1 and F_2 on Pt-1Pd surface

system	surface					
	Pt^S-Pt^S	Pt^S-Pt	Pt-Pd	Pt^S-Pd	Pt^S-S	Pd-S
F_1	0.24		0.17		0.51	
F_2	0.24	0.53	0.12	-0.13	0.53	0.27

[s] Atom of connecting with S atom. [a] the second atom.

We calculated the Hirshfeld atomic charges for different atoms after S adsorption on metal surface as shown in Table 6. When S is adsorbed on the Pt(111) surface, the electronic charge of surface Pt atom connecting with S atom is decreased 0.033e^-. S

atom gains a negative charge 0.020e^-, so there is transference of electron density from the Pt of surface atoms to the adsorbed S atom. When S is adsorbed on the Pt-nPd(111) (n =1-3) surface, the electronic charge of surface Pt atom is reduced about 0.039e^- ,0.052e^- and 0.069e^- comparing with the clean alloy surface, respectively. The electronic charge of Pd atom has a small decrease, especially the Pd atom connecting with the S atom. The electron transference towards S atom is 0.040e^-, 0.088e^- and 0.137e^- (more than on Pt (111) surface), respectively. When S is adsorbed on the Pt-4Pd (111) and Pd (111) surface, the electronic charge of surface Pd atom connecting with S atom decreases 0.07e^- and 0.073e^-. The electron transference toward S atom (0.189e^- and 0.190e^-) is higher than in the previous case. The electronic charges of second layer atoms have increase when S is adsorbed on (111) surface.

Table 6. Charges for S, surface Pt and Pd, 2nd layer Pt atoms for S at F_1 site on Pt-nPd(111) (n =1-4).

System	Atom	Charge
S/Pt	Pt^S	0.017(-0.016)
	Pt	-0.027(-0.016)
	Pt_a	-0.04(0.013)
	S	-0.020(0)
S/Pt-1Pd	Pt^s	-0.029(-0.068)
	Pd	0.187(0.190)
	Pt_a	-0.015(0)
	S	-0.040(0)
S/Pt-2Pd	Pt^s	-0.070(-0.122)
	Pd^s	0.189(0.148)
	Pd	0.150(0.148)
	Pt_a	-0.028(-0.014)
	S	-0.088(0)
S/Pt-3Pd	Pt^s	-0.111(-0.180)
	Pd^s	0.153(0.099)
	Pd	0.112(0.099)
	Pt_a	-0.043(-0.030)
	S	-0.137(0)
S/Pt-4Pd	Pd^s	0.117(0.047)
	Pd	0.072(0.047)
	Pt_a	-0.058(-0.048)
	S	-0.189(0)
S/Pd	Pd^S	0.060(-0.013)
	Pd	0.008(-0.013)
	Pd_a	-0.002(0.011)
	S	-0.190(0)

$_a$ Second layer atom. ^{s} atom of connecting with S atom. Values in parentheses are charges of no adsorption.

The PDOS of HS adsorbed at the B_1 and B_2 sites on Pt-1Pd surface is given in Fig. S1 of the Supporting Information. The same as S adsorption, d states of Pt or Pd atom spread out into lower energies and broaden, where the electron density overlaps with the p states of S. In Fig. S1a, the two overlap areas of the density of states are about -12.5 and -19.8 eV, respectively, are lower than in Fig. S1b (about -12.3 and -19.4 eV, respectively), indicating a stronger interaction between the HS and surface when HS is adsorbed at the B_1 site.

The PDOS of H_2S adsorbed at the T_1 and T_2 sites on Pt-1Pd surface is shown in Fig. 5. The H_2S molecule possesses C_{2v} symmetry; four valence states of H_2S are marked 4a1, 2b2, 5a1, and 2b1 according to their orbital symmetries. The PDOS indicates that states 4a1 and 2b1 are contributed mainly from atomic orbitals 3s and 3p of the S atom, whereas 2b2 and 5a1 states arise from the hybridization of orbital 3p of the S atom and 1s of the H atom. From the Fig. 5a, we can see that the two sp states in gas phase H_2S corresponding to S-H σ bond overlap the clean surface atom d-band. After S adsorption, the S 3p electron peak broadens and is shifted to the lower energy overlapping the d-orbital states of the surface atoms which itself shifts to lower energies, especially H_2S at the T_1 site. And all S 3p atomic orbital of adsorbed H_2S have significant overlaps with the d orbital of the atom that is bound to the H_2S molecule, especially the Pt atom. This indicates that the occupancies of the metal d states and S 3p states have redistributed to an increased occupancy at lower energies due to the interaction of S and surface atoms. These results are consistent with the previous studies of H_2S adsorption on Pd-Ni and Pd-Cu alloys.[39] As shown in Fig. 5b, the overlap peak appeared at around -21.0 and -10.2 eV when H_2S on the T_1 site, lower than that of the T_2 site,-20.4 and -9.5 eV (Fig. 5c), indicating a strong interaction and more adsorption energy of H_2S on the T1

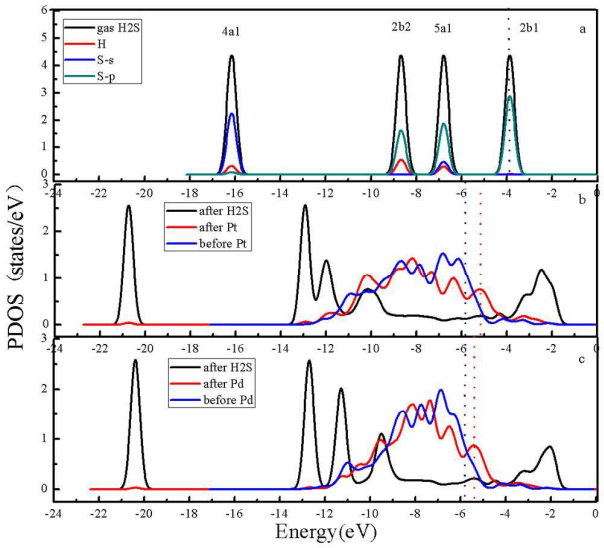

Fig. 5. PDOS of H_2S adsorption on Pt-1Pd(111): (a) gas H_2S, (b) H_2S at the T_1 site, (c) H_2S at the T_2 site.

site on the T_1 site. The calculated charges of the molecule H_2S on the T_1 and T_2 are 0.1402e^- and 0.0896e^-, respectively. The results indicate that H_2S→Pt charge transfer is stronger than that of H_2S→Pd. From the above the analysis, we can conclude that the interaction of H_2S with Pt atom is stronger than that of the Pd atom, explaining the fact that the T_1 site is more stable than T_2 for the adsorption of H_2S.

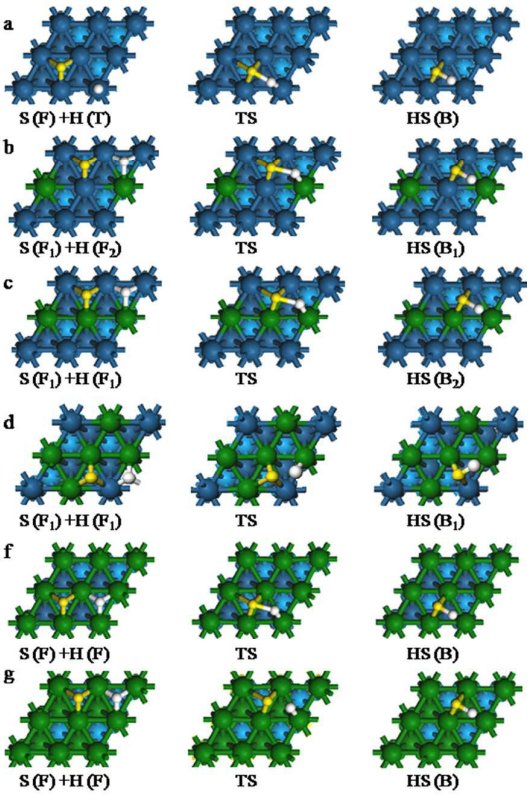

Fig. 6. Basic structures of the initial, transition and final states for S+H→HS path(I) reaction. (a) On Pt(111), (b) On Pt-1Pd(111), (c) On Pt-2Pd(111), (d) On Pt-3Pd(111), (f) On Pt-4Pd(111), (g) On Pd(111).

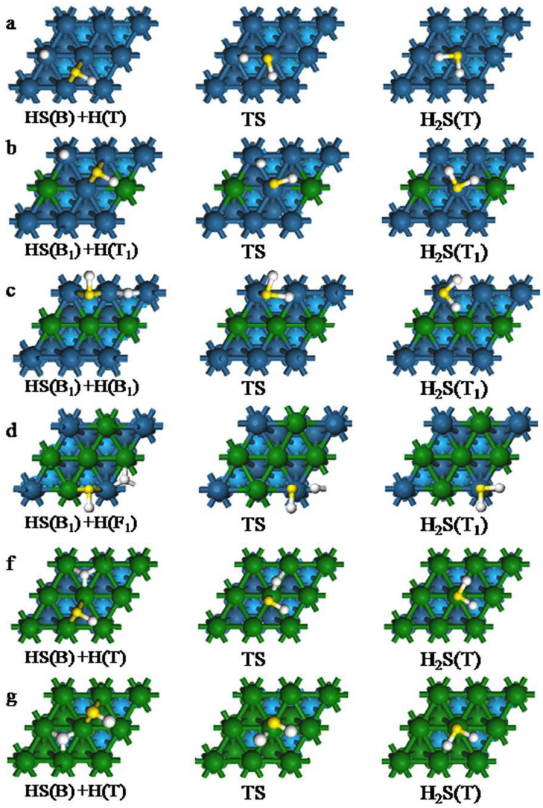

Fig. 7. Basic structures of the initial, transition and final states for HS + H→ H_2S path(I) reaction. (a) On Pt(111), (b) On Pt-1Pd(111), (c) On Pt-2Pd(111), (d) On Pt-3Pd(111), (f) On Pt-4Pd(111), (g) On Pd(111)

3.4 Hydrogenation of Sulfur

After determined the preferable adsorption sites for S, HS, H_2S and H, we also explore the possible reaction pathways for the full hydrogenation of S to H_2S. Because alloys break up the homogeneity of the surface, modelling surface reactions on alloys is more complex than on pure metals.[40] Thus, only the important reactions are considered. The vibrational frequencies of all transition states are listed in Table S1 of the supporting materials.

S + H→HS: This first step of the S hydrogenation starts with the S atom at the F site and H atom at the T site on Pt(111) surface and Pd(111) surface. On Pt-nPd(111) (n=1-3) surface, two possible reaction pathways have been explored to understand the effect of Pd atom due to the adsorption energies of the two coadsorption system have a little difference (0.02~0.07 eV). The S atom adsorbed at the F_1 site and the F_2 site in path(I) and in path(II), respectively. The IS, TS and FS corresponding to the S+H→HS reaction path on the different surfaces are shown in Fig. 6. The figure include the reaction path(I), while the reaction path(II) are given in Fig. S2 of the Supporting Information on Pt-nPd(111)(n=1-3). The reaction barriers, reaction energies along with selected geometric parameters at TS are listed in Table 7. In the S + H→HS, the reactions proceed by divalent S diffusing from the fcc site to the bridge site and H moving towards the S. The TS is reached when the distance between the H and S is d_{S-H} < 1.779 Å. After the TS, S and H combine to produce HS chemisorbed on the B site.

Our calculation demonstrates that the reactions on different surfaces are all endothermic and the predicted energy change varies from 0.35 to 0.65 eV. The barrier is found to be moderately higher on Pt(111) and the path(I) of the Pt-nPd(111) (n=1-2). On Pt(111), the reaction energy of S hydrogenation is 0.65 eV which is 0.10~0.20 eV higher than on Pt-Pd alloys metal and Pd(111). On Pt-nPd(111) (n=1-2), the barrier of the path(II) is 0.72 and 0.74 eV, respectively, which is lower than that of the reaction path(I). On the different alloy surfaces, the transition states are structurally more product-like than reactant-like. At the transition state, the S-H distance is 1.625~1.779 Å, longer by 0.235~0.404 Å compared to the product. For the S-Pt and S-Pd corresponding bond length are 2.331~2.357 Å and 2.313~2.343 Å , and they are reduced by 0.01~0.05 Å.

HS+H→H_2S: HS hydrogenation starts with HS on the B site and H on the adjacent stable site. On Pt-nPd(111) (n =1-3), there are also two corresponding reaction pathways due to thecoadsorption energy of HS and H is litter different, less than 0.06 eV. The IS, TS and FS corresponding to the HS+H→H_2S reaction path(I) on the different surfaces are shown in Fig. 7, and structures of the raction path(II) are given in Fig. S3 of the Supporting Information on Pt-nPd(111)(n=1-3). In path(I), HS is at the B_1 site while the B_2 site for path(II). The reaction begins with HS and H coadsorded on the metals surface. The isolated H moves toward S of HS and monovalent HS diffuses from the B site to the

T site. After the TS, the H_{ads}-HS distance decreases further, yielding H_2S chemisorbed on the T site. The reaction energy are vary from 0.62 to 0.67 eV and 0.58 to 0.85 eV in path(I) and path(II), respectively. The S-H distance of the final states is shorted by 0.269~0.947 Å compared to the transition states. On Pt(111) and Pd(111), the reaction are also endotheric by 0.44 and 0.42 eV, with the barriers of 0.59 and 0.79 eV. In TS, the S-H bonds are 1.366 and 1.365 Å, respectively. From our calculation, S and HS must be activated from the preferred chemisorption site in order to achieve a transition state for the studied metal in both S+H→HS and HS+H→H_2S reactions. During this process, S and HS must move from the F and B site to the B and T site, respectively. This is coincident with Michaelides et al.[41]

To determine whether the incorporation of Pd into Pt could increase the ability of the catalyst to hydrogenation reaction of S, we need to consider how the alloying affects the following: (a) the overall reaction energy, (b) the energy change associated with each step, and (c) the activation energy barriers. This can be done by comparing the energetic pathways for each of the metal surfaces.[34] A detailed energy profile for the hydrogenation reaction of S is presented in Fig. 8. The hydrogenation of the adsorbed S and H to H_2S is a quite difficult process due to its overall endothermicity of > 2.00 eV on the different alloy surface. The energy of the overall reaction significantly decreased by 0.30~0.55 eV comparing with pure Pt(111) due to doping Pd. This suggests that the addition of Pd into Pt can improve the reactivity for the hydrogenation of S. In the S+H→HS reaction, the barrier of all Pt-Pd alloys decrease except for the path(I) on Pt-2Pd(111) compared to the Pt(111). In the HS+H→H_2S reaction, there are lower barrier on Pt-1Pd (111). As shown in Table 7, the barriers of Pt-1Pd(111) are 0.58 and 0.62 eV almost equalling with on Pt(111). From above analysis, we can see that Pt-1Pd alloy will enhance the active of the catalyst and promote the hydrogenation reaction of S.

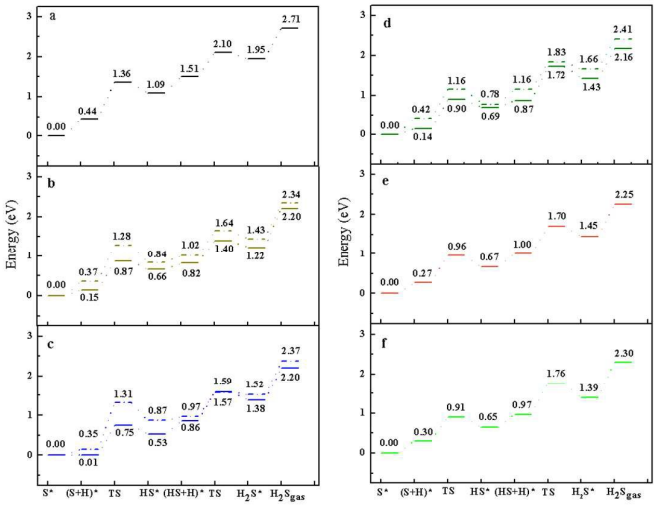

Fig. 8. Potential energy surfaces for the hydrogenation of S on (a) Pt(111), (b) Pt-1Pd(111), (c) Pt-2Pd(111), (d) Pt-3Pd(111), (e) Pt-4Pd(111), (f) Pd(111). Dot dash line and straight line represents Path I and Path 2, respectively.

Table 7. Reaction barrier (E_a), reaction energy (ΔE) and geometric parameters at the transition state for hydrogenation of S reaction on reactions on the different metal surfaces (values in parentheses refer to the final state).

reaction	E_a(eV)	ΔE(eV)	d_{S-H}(Å)	d_{S-Pt}(Å)	d_{S-Pd}(Å)
Pt					
S + H → HS	0.92	0.65	1.641(1.377)	2.357(2.380)	
HS+ H → H_2S	0.59	0.44	1.906(1.366)	2.332(2.386)	
Pt-1Pd					
S(F_1) + H → HS	0.91	0.47	1.779(1.375)	2.356(2.370)	
HS (B_1) + H → H_2S	0.62	0.41	1.803(1.367)	2.345(2.372)	
S(F_2) + H → HS	0.72	0.51	1.711(1.376)	2.337(2.371)	
HS (B_2) + H → H_2S	0.58	0.40	1.733(1.367)	2.362(2.370)	
Pt-2Pd					
S(F_1) + H → HS	0.96	0.52	1.764(1.375)	2.336(2.343)	2.343(2.414)
HS (B_1) + H → H_2S	0.62	0.55	1.746(1.367)	2.388(2.358)	
S(F_2) + H → HS	0.74	0.52	1.626(1.376)	2.336(2.348)	2.376(2.414)
HS (B_2) + H → H_2S	0.71	0.52	2.315(1.368)	2.334(2.355)	
Pt-3Pd					
S(F_1) + H → HS	0.74	0.36	1.752(1.377)	2.331(2.341)	2.332(2.404)
HS (B_1) + H → H_2S	0.67	0.50	1.812(1.364)	2.413(2.401)	
S(F_2) + H → HS	0.76	0.55	1.625(1.373)		2.352(2.379)
HS (B_2) + H → H_2S	0.85	0.56	1.631(1.362)		2.344(2.388)
Pt-4Pd					
S + H → HS	0.69	0.40	1.746(1.376)		2.313(2.369)
HS + H → H_2S	0.70	0.45	1.810(1.365)		2.482(2.373)
Pd					
S + H → HS	0.61	0.35	1.747(1.377)		2.324(2.373)
HS + H → H_2S	0.79	0.42	2.249(1.365)		2.362(2.392)

The lower barriers on the Pt-1Pd(111) indicate that the hydrogenation reaction should proceed at lower temperatures. However, the reverse reaction dehydrogenation on Pt-1Pd(111) from $H_2S \rightarrow H+HS$ and $HS \rightarrow H+S$ have low barriers of 0.42 and 0.21 eV in Path(I), 0.21 and 0.18 eV in Path(II), respectively. This indicates that the reverse process is more likely to occur, especially below room temperature. On Pt-1Pd(111), the reaction barrier of the path(I) is 0.91 eV which is 0.19 eV higher than the path(II) in S + H→HS reaction. The smaller barrier for path(II) can be attributed to the fact that the adsorption energy of the initial states is smaller and the weaker S–surface bond before dissociation. In the $HS+H \rightarrow H_2S$ reaction, both the barriers in the path(I) and path(II) are almost equal with each other, about 0.62 and 0.58 eV. To elaborate the most likely pathway of the S hydrogenation reaction on Pt-1Pd(111), the rate constants when S on F_1 site and F_2 site are calculated according to the previous reports, respectively.[42] We calculate that the rate constants k of the path(II) are 2.6×10^7 and 3.7×10^7, 7 and 5 orders larger than that of the path(I) in S+H→HS and $HS+H \rightarrow H_2S$ reaction at 300 K, respectively. This suggests that the rate of the path(II) in the S hydrogenation is quicker than path(I).

4. Conclusion

Density functional theory calculations were employed to investigate possible adsorption structures and the mainly reaction pathways for the hydrogenation reactions of the S at the different adsorption sites on Pt(111), Pt-nPd(111) (n=1-4) and Pd(111). H_2S molecule was quite weakly adsorbed, favouring the top site and with the molecular plane lying parallel to the surface. HS and S interact strongly with the surfaces comparing with H_2S and were adsorbed preferentially on the bridge, fcc and top sites. On Pt-nPd (111) (n=1-3), the preferred adsorption site for S, HS and H_2S was on the F_1, B_1 and T_1 sites, respectively. H was preferentially adsorbed on the T and T_1 site On the Pt(111) and Pt-nPd(111) (n=1-3), respectively. While on Pt-4Pd(111) and Pd(111), H was preferentially adsorbed on the F site. The adsorption energy of S, HS, H_2S and H was weaker on Pt(111) than on Pt-nPd(111) (n =1-4). It has been found that Pd atom has a lower attraction to S, HS, H_2S and H compared to Pt atom. PDOS analysis indicated that the width of the occupied portion of the d-band of Pt atom is wider than Pd atom. Pt atom and adsorbate have significant overlapping than Pd atom.

Our calculation demonstrated energy barriers for the formation of HS on the Pt-Pd(111) alloy surface are lower than on Pt(111). We think the result is due to the new sites with high hydrogenation activity were probably created in the Pt-Pd catalyst. The energy of the overall reaction significantly decreased on Pt-Pd alloy surface comparing with pure Pt(111), suggesting the lower energy for the hydrogenation reaction. From the above, the Pt-Pd alloy catalysts enhanced the hydrogenation activity. On Pt-1Pd(111), there are two reaction paths, the reaction barrier of the path(I) is 0.91 eV which is 0.18 eV higher than path(II) in the S+H→HS reaction. In the $HS+H \rightarrow H_2S$ reaction, both the barriers in the path(I) and path(II) are almost equal with each other, about 0.62 and 0.58 eV. From our calculated potential energy surfaces and the rate constant, the path(II) would be preferable in theory. However, adsorption energy of S at the F_1 is larger than that for S at the F_2 site, making the reaction of the path(I) might show its possibility as a competitive pathway.

This theoretical work provides a systematic study to understand the effect of alloying elements, by analyzing the adsorption energy, electric structure and hydrogenation reaction. Our calculation results show that Pt-Pd alloy catalysts, especially Pt-1Pd catalyst, can enhance the hydrogenation activity of S. This could provide the guide to the development of highly active catalysts.

Acknowledgements

This work is supported by the National Natural Science Foundation of China (Grant No. 51502348) and the Fundamental Research Funds for the central Universities (14CX05038A and 13CX02018A).

References

1 B. C. Gates, *Catal. Chem*, 1992, *Wiley: New York.*
2 R. I. Masel, Principles of Adsorption and Reaction on Solid Surfaces, 1996, *Wiley: New York.*
3 M. Kiskinova, *Surf. Sci. Rep,* 1998, **8**, 359.
4 D. W. Goodman, *J. Phys. Chem*, 1996, **100**, 13090.
5 L. I. Ali, A. A. Ali, S. M. Aboul-Fotouh, A. K. Aboul-Gheit, *Appl. Catal. A*, 1999,**177**, 99.
6 V. G. Baldovino-Medrano, S. A. Giraldo and A. Centeno, *Fuel*, 2010, **89**, 1012.
7 J. R. Chang, S. L. J. Chang, *Catal*, 1998, **176**, 42.
8 C. Song, A. D. Schmitz, *Energy & Fuels*, 1997, **11**, 656.
9 A. Corma, A. Martínez, V. J. Martínez-Soria, *Catal*, 1997, **169**, 480.
10 M. Vaarkamp, W. Dijkstra, B. H. Reesink, P. H. Berben, *Am. Chem. Soc. Div. Petrol. Chem. Prepr*. 1998, **43**, 77.
11 J. Lee, H. J. Rhee, *Catal*, 1998, **177**, 208.
12 H. Yosuda, Y. Yoshimura, *Catal. Lett*, 1997, **46**, 43.
13 A. Niquille-Röthlisberger, R. Prins, *J. Catal*, 2006, **242**, 207.
14 Hong Jiang, Hong Yang, Randall Hawkins, Zbigniew Ring. *Catal. Today*, 2007, **125**, 282.
15 B. J. Delley, *Chem. Phys*, 1990, **92**, 508.
16 B. J. Delley, *Chem. Phys*, 1996, **100**, 610.
17 X. Q. Gong, A. Selloni, M. Batzill and U. Diebold, *Nat. Mater.* 2006, **5**, 665.
18 J. P. Perdew, Y. Phys. Wang, *Phys. Rev. B*, 1986, **33**, 8800.
19 J. P. Perdew, Y. Wang, *Phys. Rev. B*, 1992, **45**, 13244.
20 R. Garćla-Muelas, Q. Li, N. Lopez, ACS Catal, 2015, **5**, 1027.
21 B. Delley, *Phys. Rev. B*, 2002, **66**, 155125.
22 H. J. Monkhorst, J. D. Pack, *Phys. Rev. B*, 1976, **13**, 5188.
23 C. Popa, W. K. Offrmans, R. A. V. Santen, A. P. Jansen, J. Phys. Rev. B, 2006, **74**, 155428.
24 B. R. Coles, *J. Inst. Met*, 1956, **84**, 346.
25 A. Michaelides, P. Hu, *J. Chem. Phys*, 2001, **115**, 8570.
26 D. R. Alfonso, A. V. Cugini, D. C. Sorescu, Catal Today, 2005, **99,** 315.
27 H.Y Zhu, W.Y Guo, R.B Jiang, L.M Zhao, X.Q. Lu, M. Li, D.L. Fu, H.H. Shan, Langmuir, 2010, **26**, 12017.
28 D. R. Papai，C. M. Salahub，Surf. Sci.，1999，**236**, 241.
29 T. A. Halgren, W. N. Lipscomb, *Chem. Phys. Lett*, 1977, **49**, 225.
30 W. F. K. Wynne-Jones, H. Eying, *J. Chem. Phys*, 1935, **3**, 492.

31 R. J. Koestner, M. Salmeron, E. B. Kollin, J. L. Gland, *Chem. Phys. Lett*, 1986, **125**, 134.

32 R. C. Shiell, X. K. Hu, Q. J. Hu., J. W. Hepburn, *J. Phys. Chem. A*, 2000, **104**, 4339.

33 J. A. Rodriguez, S. Chaturvedi, M. Kuhn, J. Hrbek, *J. Phys. Chem. B,* 1998, **102**, 5511.

34 Erik. J. Albenze, A. Shamsi, *Surf. Sci,* 2006, **600**, 3202.

35 V. Mokrushin, V. Bedanov, W. Tsang, M. Zachariah, V. Knyazev, ChemRate, version 1.5.2, *National Institute of Standards and Technology: Gaithersburg*, MD, 2006.

36 D. R. Alfonso, A. V. Cugini, D. C. Sorescu. *Catal. Today*, 2005, **99**, 315.

37 G. Papoian, J. K. Nørskov, R. J. Hoffmann, *Am. Chem. Soc*, 2000, **122**, 4129.

38 L. J. Richter, W. Ho, *Phys. Rev. B*, 1987, **36**, 9797.

39 E. Ozdogan, J. Wilcox, *J. Phys. Chem. B*, 2010, **114**, 12851.

40 M. P. Hyman, B. T. Loveless, J. W. Medlin, *Surf. Sci*, 2007, **601**, 5382.

41 A. Michaelides, P. Hu, *J. Chem. Phys*, 2001, **115**, 8570.

42 T. S. Rufael, J. Prasad, D. A. Fischer, J. L. Gland, *Surf. Sci,* 1992, **78**, 4.

ARTICLE